Current and Future Chromatographic Columns: Is One Column Enough to Rule Them All?

Broeckhoven, Ken; Eeltink, Sebastiaan; De Malsche, Wim; Matheuse, Fréderick; Desmet, Gert; Cabooter, Deirdre

Published in:
LC GC North America

Publication date:
2018

Document Version:
Accepted author manuscript

One column to rule them all? (short title)

Current and Future Chromatographic Columns: is one column enough to rule them all? (full title)

K. Broeckhoven*[,1], D. Cabooter[2], S. Eeltink[1], W. De Malsche[1], F. Matheuse[1], G. Desmet[1]

[1]**Vrije Universiteit Brussel, Department of Chemical Engineering, Pleinlaan 2, 1050 Brussel, Belgium**

[2] **University of Leuven (KU Leuven), Department of Pharmaceutical and Pharmacological Sciences, Herestraat 49, 3000 Leuven, Belgium**

*** Corresponding author: ken.broeckhoven@vub.be**

Abstract:

In this contribution, the current state-of-the-art and recent developments in column technology are discussed. The vast majority of separations in liquid chromatography still uses the typical packed particle bed format, most commonly with fully or superficially porous particles in particle sizes as low as 1.3 µm. As an alternative, monolithic columns have been the topic of a large number of studies, but are currently only used in some niche applications. Research into perfectly ordered microfabricated columns has shown tremendous possibilities for these highly performant columns for use in nano-LC, but their development is still ongoing. The possibilities that the emerging technology of 3D printing offers would make it theoretically possible to develop any imaginable structure with high precision, but is currently limited by the available spatial resolution and required printing time, narrowing the size and application range. A critical review of all these technologies is provided and demonstrates that the further development of chromatographic columns will be of paramount importance in the years to come.

1. Introduction

The improvements in instrument and column performance in liquid chromatography (LC) over the last 15-20 years have resulted in an almost 10-fold reduction in analysis time and 3-fold increase in separation efficiency. Nevertheless, the complexity of the samples emerging in life sciences (proteomics, metabolomics, lipidomics…), containing 10,000 or more analytes in a wide range of concentrations and physico-chemical properties (size, polarity, ionization state…) is so vast that it is impossible to even dream of ever achieving full resolution using unidimensional chromatography with the present state-of-the-art in instrumentation and columns. The rise of two-dimensional separation techniques, in combination with modern MS/MS systems, vastly increases the overall resolving power that can be achieved [1-4]. Nevertheless, even 2D separations are ultimately limited by the efficiency of the chromatographic column in the individual dimensions. In addition to the need for enhanced resolution, a further increase in separation speed for the 2nd dimension column is in high demand as well, as this would allow to increase the sampling rate in the 1st dimension, better preserving its resolution.

The further development of faster and more efficient LC chromatographic columns thus remains of paramount importance in the years and decades to come. In addition, also the chromatographic instrumentation will need to follow these improvements and changes in the performance and format of chromatographic columns [5].

Overall, the main factors that determine the separation power and speed of any system are given by the Knox and Saleem equation [6,7], determining the time, t, needed to achieve a given number of theoretical plates, N, under fully optimized kinetic conditions and for a given maximum pressure, $\Delta P_{max,}$ (which can be either column or instrument limited) and mobile phase viscosity, η:

$$t = \frac{\eta}{\Delta P_{max}} \cdot E \cdot N^2 \qquad (1)$$

$$\text{with } E = h_{min}^2 \cdot \phi = H_{min}^2 / K_v \qquad (2)$$

with H_{min} and h_{min} the minimum absolute and reduced plate height, respectively and K_v and ϕ the hydraulic permeability and the flow resistance of the bed, respectively. The importance of the instrumentation (pressure limit, extra column dispersion) and the effect of mobile phase viscosity (LC,GC,SFC) in this equation were discussed earlier [5,8]. The focus of the present contribution will be on the factors grouped in the so-called separation impedance E [6,7], determining the column quality. E is a dimensionless number and is hence independent of the size of the support. It only depends on its shape. In fact, the E-number represents the ability of a given chromatographic support shape to transport the mobile phase through the column with a minimum of dispersion and pressure losses. The smaller E, the smaller these losses, and hence the shorter the time needed to achieve a given N. By far the most important geometrical factor determining the value of E is the external porosity ε, essentially because of its effect on the flow resistance. Computational fluid dynamics simulations on idealized monolithic support structures with varying ε have revealed that, while the domain-size based h does not vary much when ε increases, ϕ can easily decrease with an order of magnitude when the structure becomes more open and, for example, increases from ε=40% (=porosity of the packed bed of spheres) to say ε=85% [9]. As a consequence, also E and the associated separation time (cf. Eq. 1) can be expected to drop by an order of magnitude. For an increase in ε=40% to ε=60%, ϕ is about 3 times smaller, offering 3-fold faster separations than with a packed bed. However, in order to benefit from the shorter analysis times via the reduction of E with increasing porosity, this increase should be accompanied by a significant decrease of the support size. If not, the optimal N value for which Eq. (1) holds increases as well, leading to longer analysis time. Finding ways to simultaneously increase ε and decrease the size of the support elements, while maintaining a good structural homogeneity, mechanical strength and sufficient retention surface, is the key to realize a paradigm shift in the speed and performance of LC columns.

2. Packed bed columns

The vast majority of chromatographic columns sold nowadays are filled with fully or superficially porous particles [10]. These columns show excellent reproducibility in both performance and selectivity and are available from capillary up to (semi-)preparative scale in a wide range of lengths, packed with different particle sizes and stationary phase chemistries. Whereas h_{min}=2 was long considered the practically achievable lower limit for column efficiency for analytical columns (2.1-4.6 mm I.D.), the new generation of superficially porous particles (SPP) allows to achieve h_{min} values as low as 1.4. Spurred by these developments, attempts have been made to produce fully porous particle batches with a reduced particle size distribution, such that nowadays h_{min}-values as low as 1.7 can be achieved with fully porous particles [11-14]. It should be noted that in capillary formats, h_{min}-values down to h_{min}=1 have been demonstrated in research laboratories [15].

The fact that particles in a packed bed need to be in contact with each other to obtain a stable and pressure resistant bed, makes that the external porosity ε of a randomly packed bed is always around 36 to 40%. As a consequence, the flow resistance ϕ_0 of packed beds is difficult to alter or optimize and usually lies between 600 and 800 [16,17]. In a first approximation, ϕ_0 can be calculated according to Kozeny-Karman's law (based on the u_0 velocity of an unretained t_0-marker):

$$\phi_0 = 180 \cdot \frac{(1-\varepsilon)^2 \cdot \varepsilon_T}{\varepsilon^3} \qquad (3)$$

Since ϕ_0 not only depends on ε but also on the total porosity ε_T, a clear reduction of the flow resistance is obtained when switching from fully porous to superficially or non-porous particles (lower total porosity ε_T than fully porous particles). The effect is however rather small and difficult to exploit because a reduction of the porous zone fraction of the particles reduces the sample loadability, causing efficiency loss when a large sample mass is injected [18].

The only way to further improve the kinetic performance of packed bed columns would thus be a further reduction in h_{min}. The latter can be highly effective, given the quadratic variation of E

with h_{min}. As a result of this quadratic dependency, the seemingly modest reduction of h_{min} by some 20-30% that is typically observed when moving from fully porous to superficially porous corresponds to a very significant two-fold reduction in analysis time. Using typical values for h_{min} and ϕ_0 for superficially porous (h_{min}=1.5,ϕ_0=600) and fully porous (h_{min}=2,ϕ_0=800) particle columns, E-numbers are around 1350 and 3200 respectively. These values are in good agreement with experimental results [17,19].

Further improvements in packing heterogeneity, reducing the so-called eddy dispersion contribution (A-term), are thus of high interest. As recently discussed by Gritti et al., perfectly ordered packed beds (A-term = 0) are expected to yield h_{min} values equal to 0.9,0.7 or 0.5 for fully, superficially and non-porous particle columns respectively, as it is impossible to eliminate longitudinal diffusion and mass transfer resistance contributions [13]. Finding ways to further suppress the eddy-dispersion while sticking to the traditional slurry packing methods seems to be rather difficult (Fig. 1a), if not impossible, given the many efforts already devoted to the problem in the past decades [13]. It seems that radically novel packing methods are needed. One approach, currently under investigation in our group would be the use of additive layer manufacturing, where ordered layers of monodisperse silica particles are assembled layer by layer to form a 3D printed particle column (Fig. 1b). However, this concept is still far from reality. Besides the cost efficiency, one critical aspect is the pressure stability of these beds under the very high operating pressures (up to 1500 bar) nowadays available in commercial UHPLC equipment.

An approach to lower the h_{min} of packed bed columns that appears closer to reality (given the existence of an experimental proof delivered by Wei et al.) is the production of core-shell particles wherein the mesopores are oriented purely radially instead of forming a randomly connected network. Although this seems only a small change, it has such a strong effect on the B-term that it can be expected to lead to a further reduction of 0.5 reduced h-units compared to the conventional core-shell particle performance [20,21].

3. Monolithic columns

Instead of stacks of individual particles as in packed bed columns, monolithic columns consist of a continuous porous skeleton with large through-pores (Fig. 2). Already in the early 1950's the potential of this column format was discussed by Nobel Prize Laureates Martin and Synge [22]. The in-situ synthesis of monolithic materials has several advantages, such as the absence of frits to retain particles in the column and a facilitated development of miniaturized column formats, such as capillaries (Fig. 2a,2c) and microfluidic chips (Fig. 2e). Also the use of thin monolithic layers to obtain a retentive porous layer for use in open-tubular (Fig. 2d) or pillar-array devices (Figs. 2b) has been demonstrated [23-25]. In principle monolithic stationary phases have the potential to outperform packed columns. Whereas the efficiency of packed columns is related to the particle size while the total porosity and thus flow resistance is fixed, the use of porogenic solvents in the preparation of monolithic materials facilitates the optimization of the globule size/skeleton (almost) independently of ε. The advantage that ε can be made very large (values up to ε=86% have been reported for use in liquid chromatography [26]), makes them intrinsically much better suited to obtain small E-values and a correspondingly improved kinetic performance. Silica-based capillary monolithic columns for example have been shown to produce E-values as low as 300 [27]. This quantum leap in E is entirely due to the lower flow resistance of monolithic columns (in turn a direct consequence of their higher external porosity ε), because monolithic columns can at best (i.e., when they are produced with similar degrees of eddy-dispersion) be expected to produce about the same (domain size-based) h_{min}-value as packed bed columns (cf. the small effect of ε on h_{min} in Fig. 10 of [9]).

However, an advantageous shape and a concomitantly low E-number is not everything. The absolute size of the support also matters. Here the rule is very simple: instead of creating a large external porosity by increasing the size of the through-pores, the latter should be kept constant (or even made smaller) in order to keep the same mobile to stationary zone diffusion distances. The only way to achieve the required high external porosity then consists of shrinking the size of the structural elements. This however brings about a number of problems which seem so difficult to solve they currently impede the success of monolithic columns. By far the most

tenacious problem in this respect is the so-called small domain size limit problem [28,29]. This problem originates from the fact that each monolith synthesis process inevitably displays a local variability on the size and position of the produced solid zone elements, which is at best absolute in size. This implies that the general heterogeneity of the structure will increase when smaller feature sizes are being pursued, putting a fundamental limit on the possible feature size reduction of monolithic columns.

3.1 Polymer monolithic columns

Whereas early forms of (gel-like) polymer monolithic materials collapsed when pressure was applied, rigid polymer-based monolithic materials (Fig. 2c), that are compatible with high-pressure operation, have become available since the 1990s [30,31]. The two most prominent classes of materials are the poly(styrene-co-divinylbenzene) based materials and monolithic entities based on methacrylate-ester-based precursors. Polymerization mixtures are typically prepared from mono- and oligovinylic monomers and an initiator in the presence of an inert diluent, called porogen. The porogen, typically a binary solvent mixture, is selected based on their ability to dissolve the monomers, yielding a homogenous solution. During the course of the polymerization reaction microgel particles are formed, following interparticle reactions via pendant vinyl groups leading to the formation of microgel clusters [32]. Ultimately, a microscopic porous network is formed, and a phase separation occurs. Details of how the reaction conditions affect the size of the microglobules and resulting macropore structure can be found in literature [33,34]. To advance the kinetic performance of monoliths, Vaast et al. described the development of nanostructured high-porosity monolithic supports allowing for sub-min peptide separations [35]. Furthermore, he linked the effects of macropore and microglobule size, and structure homogeneity, to the separation performance measured in gradient elution, both in terms of peak capacity and gradient plate height [35].

Polymer-monolithic stationary phases have emerged as an attractive alternative for packed columns in the field of biomolecule separations and their potential has been demonstrated for a wide range of biomolecules [36,37]. In reversed-phase gradient mode, ultra-fast separations (< 1 min gradients) of intact proteins have been realized in both large I.D. columns and using

capillary column formats [35]. Using a 250 mm long capillary monolithic column and applying a 2h gradient, intact proteins, including protein isoforms arising from various amino-acid modifications, were resolved yielding a maximum peak capacity of 650 [38]. Fig. 3 shows the separation of an *E.coli* digest using a 1 m long monolithic column yielding a peak capacity in excess of 1,000 [39]. To further extend the kinetic performance and applicability of monolithic columns, different innovative approaches are being currently explored, such as composite cryopolymers [40] or the incorporation of nanoparticles to extend monoliths with only reversed-phase functionalities to ion-exchange [41]. These nanoparticles might also act as structure directing agents to improve kinetic performance.

Although excellent results can be obtained for the separation of larger biomolecules, the plate numbers achieved for small-molecules on polymer-monolithic columns are typically one order of magnitude lower than that obtained on classical packed columns. Whereas the C_{18} layer on modified silica particles is extremely thin and hence the diffusion distance is short, it has been speculated that small molecules can penetrate into the polymer globules of monolithic materials, and excessive dispersion is a result of 'surface diffusion' [42].

3.2 Silica monolithic columns

Silica monoliths (Fig. 2a) are produced via a sol-gel process wherein alkoxysilanes are hydrolyzed and then polycondensed in the presence of a water-soluble porogen [43, 44]. Siloxane oligomers formed during successive condensation reactions link together to form a gel network. Spinodal decomposition occurs and phase separation takes place between the silica-rich and solvent-rich phase, forming the future silica skeletons and through-pores, respectively. Similar to polymer monoliths, the phase separation and the pore size of the gel are controlled by varying the concentration of the porogen. The stiffness and strength of the gel are increased by aging in a siloxane solution and mesopores are formed by adding ammonium to the aging solution. Finally, the gel is dried and clad with polyether ether ketone (PEEK) to obtain a silica monolith suitable for chromatographic purposes. This column housing however limits the maximum operating pressure in analytical scale columns to HPLC-like operating pressures

(generally below 400 bar), while it has recently been shown the silica monolithic skeleton itself can withstand pressures up to at least 800 bar [45].

For analytical scale monoliths (2.1-4.6 mm I.D.), through-pores sizes are typically d_{tp}= 1-2 µm and high external porosities (ε > 60%) are obtained. Due to their intrinsic high permeability, silica monoliths can be operated at high linear velocities, or in long (coupled) columns, resulting in extremely high efficiencies [46]. The small size of the silica skeletons (typically d_{skel}= 1-2 µm) results in efficiencies comparable to those obtained in columns packed with 5 µm particles, especially when operated at high flow rates [47]. However, due to the poor radial homogeneity, which can be related to their fabrication process, concomitant high eddy dispersion and their limited pressure resistance, silica monoliths [48] have not been able to compete with the particle-packed columns (sub-2 µm or sub-3 µm core-shell) that were developed around the same time [49-51]. To improve their performance, efforts have been made to improve the radial homogeneity while at the same time reducing their feature sizes by adjusting the preparation process (e.g. concentration and porogen type). This has resulted in the introduction of the so-called second generation of silica monoliths [27,52,53]. Due to their improved radial homogeneity and reduced skeleton (d_{skel}<1 µm) and through-pore sizes (d_{tp}=1.1-1.2 µm), H_{min} values are much lower compared to the first generation, and comparable to what can be obtained in 3-3.5 µm particle packed columns [54]. The downside of these reduced feature sizes is that the permeability of the monolithic column decreases accordingly, from $K_{v0}=4.7\cdot10^{-14}$ m² and $K_{v0}=4.0\cdot10^{-13}$ m² for the first generation [26,27,55] to significantly smaller values $K_{v0}=2.0\cdot10^{-14}$ m² for the second generation [55]. According to Deridder et al., the permeability of a silica monolith is directly related with the square of its skeleton size, while a more complex relation between permeability and external porosity exists, depending on the geometry of the monolith [56]. Considering that external porosity values measured for first and second generation monoliths are largely the same, the decreased permeability of the second generation monoliths must therefore mainly be attributed to the reduced skeleton and through pore sizes [55]. Nevertheless, the lower permeability of the second generation monoliths is still well above those measured for sub-3 µm particle columns.

Comparing silica monoliths with packed bed columns, similar E-values (at the lower end of the range) as for fully porous particles columns are found, with E=2200-4600 and 2200-3400 for the first and second generation, respectively [55]. To compare the separation power for a given separation problem, the kinetic plot method is a useful alternative to the impedance, as it represents the maximum plate count obtainable in a certain analysis time. Fig. 4 compares the kinetic performance for first and second generation monoliths with ΔP_{max}=200 bar. It is clear that second generation monoliths perform better (1.5-2.5x faster for a certain N) than the first generation monoliths for N<50.000. For more challenging separations (N > 50.000), the first generation monoliths perform better as their large permeability allows them to be used in longer columns without compromising the separation speed [55]. Comparing their performance with a 2.7 µm superficially porous particle packed column, operated at its own ΔP_{max}=600 bar, shows that the SPP-based column outperforms both generations of monoliths over the entire range of practically relevant plate counts. A similar conclusion can be drawn when comparing silica monoliths with sub-2 µm particle columns with ΔP_{max}=1000-1500 bar [57]. Further improvements in the structural size and homogeneity of the silica monoliths by improving their production process, together with the development of higher pressure-resistant material to clad the monolithic columns, are required before the monolithic columns can become competitive with the current state-of-the-art in particle packed column technology.

In capillary formats, the radial variation in external porosity (and hence in flow resistance) caused by the inevitable post-synthesis shrinking process is much smaller than in analytical bore columns. Producing silica monoliths with a domain size of about 2 µm in 100 µm columns, H_{min}-values as low as 4.1-4.4 µm have been demonstrated [58]. This is however still around two times larger than the lowest H_{min} ever reported for packed bed columns (H_{min}=2 µm when using 1.3 µm core-shell particles) [59]. This shows a further significant decrease of the domain size of silica monolithic columns is still needed.

4. Microfabricated columns

Pillar array columns were introduced in 1998 by Fred Regnier and co-workers as an ordered alternative to disordered chromatographic packings [60,61]. Because the packing was originally intended for capillary electro-chromatography separations requiring non-conducting substrates, the first experiments were carried out using columns produced in fused silica and PDMS. Because these substrates do not easily allow fabrication of pillars with sidewall slopes close to 90°, the substrates had to be replaced by silicon by other researchers in follow-up studies before the predicted absence of eddy dispersion due to the perfectly ordered structures was indeed reflected in the measured van Deemter curves. The first reversed-phase separations on silicon micro-pillar arrays were reported in 2007 [62], showing plate heights as low as 4 µm for retained components in a non-porous pillar bed. These initial results were obtained by measuring the band broadening in the center of the beds, i.e., by excluding the sidewall region where the flow resistance of the bed was different from that in the rest of the bed. Using computational fluid dynamics simulations this problem could be solved and appropriate designs for the side-wall region were proposed [63]. One particularly useful solution were radially elongated pillars (REP, Fig. 5g) having a lateral to axial aspect ratio larger than 10 [64-66]. The use of (at least a number of rows of) such REP structures in the flow distributors (Fig. 5f) at the inlet and outlet sections of the bed also proved to be essential to interface the columns with the outer world [67]. These distributors were also key to produce sufficiently long columns on the (relatively limited) surface of a silicon wafer, connecting different channel tracks using low dispersion turns (Fig. 5b). An interesting alternative approach was implemented by Isokawa *et al.* [68], who designed a dedicated curve and pillar bed with varying density to minimize dispersion, while at the same time increasing permeability in the turn zone.

In 2017, the first generation of a pillar array columns was introduced, consisting of a 2 m long pillar bed with 5 µm diameter pillars, spaced 2.5 µm from each other (width 315 µm, depth 18 µm, porous layer of 200 nm) (Figs. 5a-5c). This column has the permeability of a 10 µm packed bed (i.e. 2.7 10^{-13} m^2), while it produces plate heights comparable with 3-4 µm porous spherical beads (i.e. 5-7 µm) [67]. The corresponding E-number is on the order of 50 to 100, i.e., more

than an order of magnitude less than in packed bed columns. The pressure tolerance of more than 400 bar would even allow to construct columns of more than 10 m, producing more than 1.5 M plates under retained conditions (small molecules like phenones) in about half a day (12h). A lot of efforts were put in the conformal integration of porous layers into the chips, in order to increase the specific surface of the non-porous pillars. Two methods that additionally allow tuning of the pore geometry have been developed to this end and have been applied for 2.5 µm pillar spacings [24,69]. With electrochemical anodization (silicon) pores are grown inside the silicon pillar (Fig. 5d-5e), leaving the contour of the pillar unaltered [69], whereas with the sol-gel deposition technique a porous glass layer is grown on the pillar (Fig. 2b), thereby increasing the size of the pillar [24]. For some applications, such as ion-pair reversed-phase chromatography of nucleotides [70] or hydrodynamic chromatography [71], it is actually preferred that the pillars are non-porous (Fig. 5b) [72]. In this case, the plate count roughly doubles [73]. These columns have an equivalent cylindrical diameter of around 80 µm, which is a typical targeted diameter to achieve optimal flow rates for ESI-MS detection. These column features make the 1st generation of commercial pillar array columns extremely suited to achieve peak capacities > 1000 in the nano-LC flow rate range.

Since this 1st generation still uses relatively large pillars (5 µm) great improvements in both speed and efficiency can be expected when new generations will be produced with pillar diameter and spacing of the same order as the current sub-2µm particles used in packed bed columns. Technologically this is feasible, given the Bosch etching technology has the potential to achieve even sub-micron resolution [63]. Sidewall effects might appear again, but this could be countered by using REP structures that are insensitive to this effect [65].

5. 3D-printed columns

In the last decade, almost every field in scientific research has started to use 3D printing or additive manufacturing. Compared to traditional manufacturing technologies, 3D printing offers the possibility to use the full three-dimensional fabrication potential to freely tune and fabricate any favorable geometry. For applications in chromatography, 3D printing especially holds the

promise of providing a way to produce perfectly ordered structures, thus allowing to eliminate any eddy-dispersion contributions. Similar to micro-fabricated columns, the external porosity and thus the flow resistance can freely be tuned within the range where mechanically stable structures can be printed. Combining 3D printing with computational fluid dynamics simulations can lead to the design of “fully optimized” stationary phases, having limited diffusion and a low resistance to mass transfer. Another asset of 3D printing is the fast manufacturing of prototypes, making rapid iterative device development possible. The use of additive manufacturing should not be limited to stationary phases, as complete chromatographic columns (containing stationary phase, column wall, flow inlet and frits) can be fabricated simultaneously. Combining 3D printed columns with printed valves, micropumps, connectors and other microfluidic parts [74], one can even dream of producing a complete 3D printed chromatographic system on a chip.

The emerging possibilities of 3D printing have already reached the field of HPLC as could be seen at the latest HPLC conferences. In 2016, Brett Paul and co-workers showed the possibilities to fabricate 3D metal printed chromatographic columns, which were functionalized in-situ with a thermally polymerized monolith [75]. Instead of using 3D printing to obtain a scaffold on which a stationary phase is deposited, the whole column, including walls, can be printed in one step, as shown by Fee et al.. They exploited the full 3D-potential of additive manufacturing, printing both octahedral beads in a simple cubic configuration (apothems of 113.6±1.9 µm), and monolith hexagonal channels, both in parallel and herringbone arrangements (apothems of 148.2±2.0 µm) [76]. In 2017, his group printed a broad range of particle shapes including tetrahedral, octahedral, stellar octangular, triangular bipyramid and truncated icosahedra particles, in different geometric arrangements as simple cubic, body-centered cubic and face-centered cubic [77]. However, for 3D printing to become the new standard of column manufacturing, some significant disadvantages need to be overcome. The most important hurdle is the resolution or minimal printed feature size, being around 25-100µm for the most widespread technologies, such as extrusion based printing (Fused Deposition Modeling), stereolithography (Stereolithographic Apparatus, Digital Light Processing), and powder-based printing (Selective Laser Melting, Selective Laser Sintering, inkjet-based printers) [74]. State-of-

the art packed bed column technologies with e.g. sub-2µm particles have feature sizes (flow-through pores) in the order of 500nm and below. Currently, only one additive manufacturing technology exists which offers competitive resolutions, namely two-photon polymerization printing (2PP). Nevertheless, other 3D print technologies with lower resolutions can be applied for the manufacturing of preparative columns, not being so demanding towards micron-scale feature sizes. A 2PP printer operates by emitting near-IR femtosecond pulses of photons into a photo-polymerizable resin. Two photons need to be simultaneously absorbed to initiate radical polymerization, a process so rare that it only takes place in the focal spot size of the laser, leading to extremely small voxel (volume-pixel) sizes. With minimal feature sizes smaller than 50nm [78], stationary phases with characteristic distances of 1µm size can thus be manufactured with high accuracy (see Figs. 2f and 6). A drawback of 2PP however is the trade-off between high resolution and printing time/volumes. Whereas new structures can be quickly prototyped in manifold with all other 3D print technologies, the speed of (mass-)production with 2PP still has a long way to go. The manufacturing of a structure as shown in Fig. 2f (ε=80%, edges of 1µm, through pores of 1.5µm) for a 1cm long column with a width of 100µm and 10µm deep (equivalent to a 40µm ID capillary) takes almost 1 day to print. It needs to be mentioned that printing time is highly influenced by the spatial dimensions, structure, material choice, laser objective, writing direction and many other parameters. In addition, 2PP is much more expensive than the more widespread technologies.

Another important hurdle is the material choice, as the final obtained structure needs to be temperature and solvent resistant (e.g. no swelling). In addition, these materials will have to be functionalized to obtain an appropriate retentive surface chemistry (e.g. C_8, C_{18}, phenyl, amide…), to such an extent that no undesired interactions are possible with the starting material. As typical 2PP printed material have no inherent porosity, either the printed structure will need to be modified to create mesopores or a porous layer will need to be deposited on the surface of the printed structure to obtain sufficiently high retention surface.

6. Conclusions:

Despite the many research efforts on novel column technologies, packed columns still are the first choice in liquid chromatography. Monolithic columns are rather employed in niche applications or for their flexible applicability and possible in-situ generation in complex geometries. Further improvements in the production process of the silica-gel monoliths should aim at reducing the domain size further while maintaining or further improving the homogeneity before they can ever become competitive with the current state-of-the-art particle packed columns. The development of a suitable ultra-high pressure column housing is another issue. Polymeric monolithic columns show great potential for the separation of large (bio)molecules but have inherent disadvantages for small molecule separations. The first generation of microfabricated pillar array shows promising results for separations that require high resolving power, but reduced feature sizes are required to further enhance separation speed and efficiency. 3D printing shows a tremendous intrinsic potential for the fabrication of chromatographic columns, but the current printing hardware either does not allow to obtain the desired resolution (sub-µm) or requires too long printing time, limiting the technology at this moment to either preparative scale separations or the development of chip-scale devices. These novel developments clearly show that we have not yet reached the end of column development and further improvements can be expected in upcoming decades.

Figure Captions

Fig. 1: (a) SEM image of monodisperse particles in a random sphere packing showing the inherent packing heterogeneities; (b) artist's impression of packed bed column made using additive layer manufacturing, with monodisperse particles assembled layer by layer to form a 3D printed particle column.

Fig. 2: SEM images of (a) silica monolithic column, (b) silica monolithic layer deposited on REP column [24], (c) polymer monolithic column, (d) silica monolithic layer deposited on capillary column for use in open tubular LC [23], (e) silica monolithic column synthesized in pillar array column [25], (f) 3D printed monolithic column. Figures adapted from refs., with permission.

Fig. 3: High-resolution LC-MS/MS analysis of a tryptic digest of E. coli obtained on a 1 m long monolithic column. Adapted from ref. [39], with permission.

Figure 4: Kinetic plots of analysis time (t_R) versus plate count (N) for benzophenone and for first generation monoliths (◊ and Δ) and second generation monoliths (■ ◆ ● ▲) evaluated at 200 bar. Open, blue symbols refer to first generation monoliths, closed, black symbols to second generation monoliths. The red curves (×) are obtained for a core-shell column (2.0x100mm, dp=2.7 µm) operated at a maximum pressure of 600 bar. The mobile phase was adapted on all columns to obtain k=8.7 for benzophenone. Adapted from [55], with permission.

Fig. 5: (a) Silicon waver featuring several pillar array columns, with zoom in on (b) turn structures at the end of each channel to increase total column length, (c) cylindrical pillars making up the chromatographic bed, (d) anodized pillars to increasing retentive surface [67], (e) detail of porous shell [67], (f) channel inlet flow distributor; (g) alternative bed structure with radially elongated pillars [65]. Figures adapted from refs., with permission.

Fig. 6: Example of a 3D printed tetrahadron skeleton model type bed (zoom: see Fig. 2f).

Figure 1:

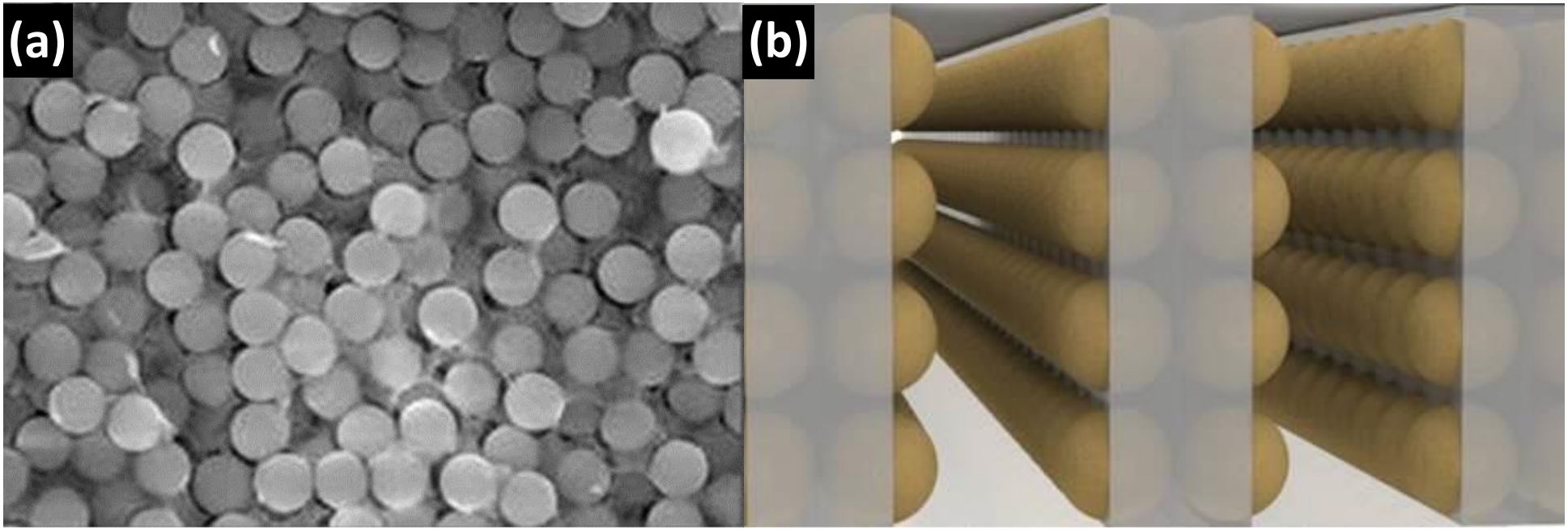

Figure 2:

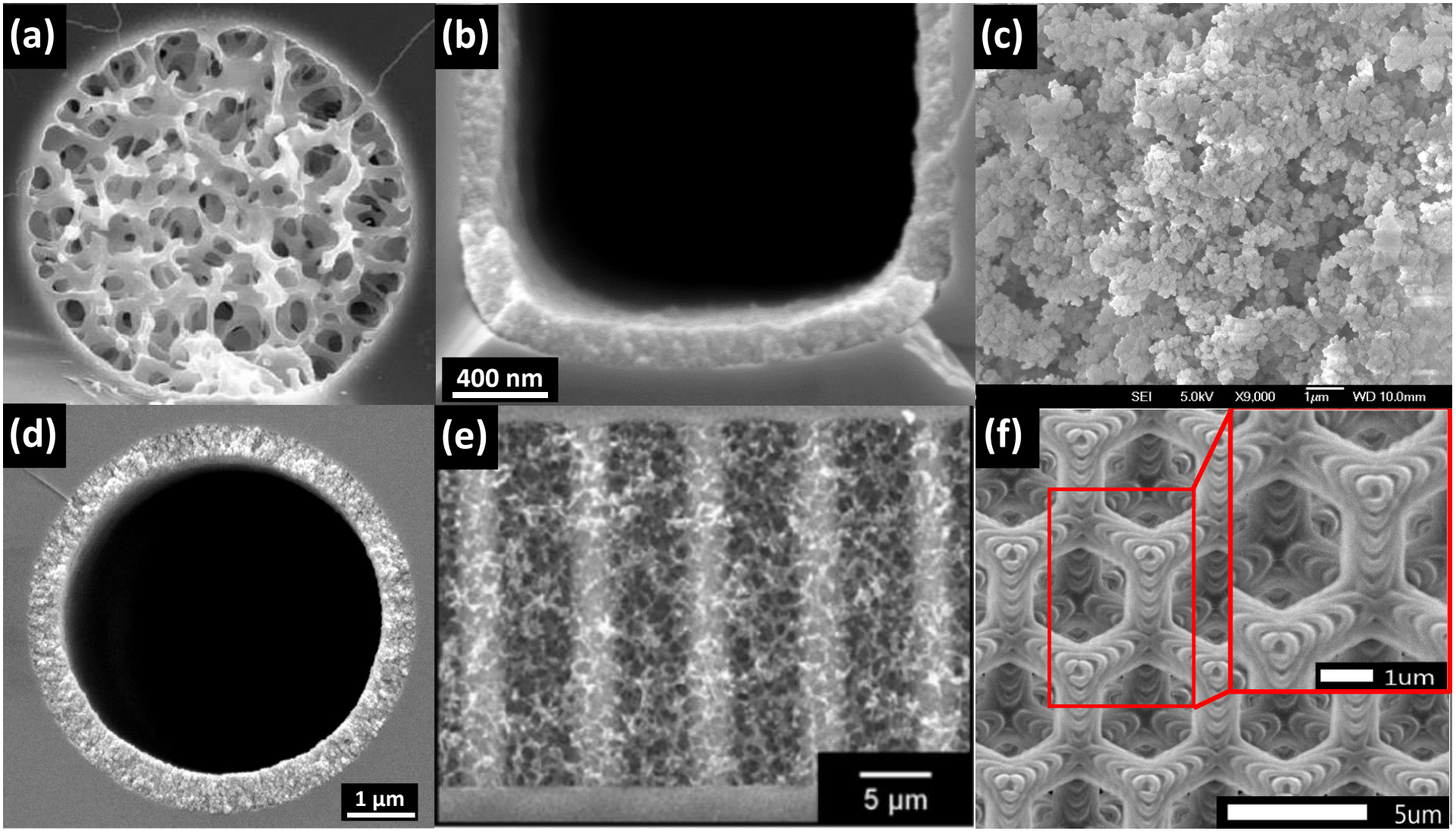

Figure 3:

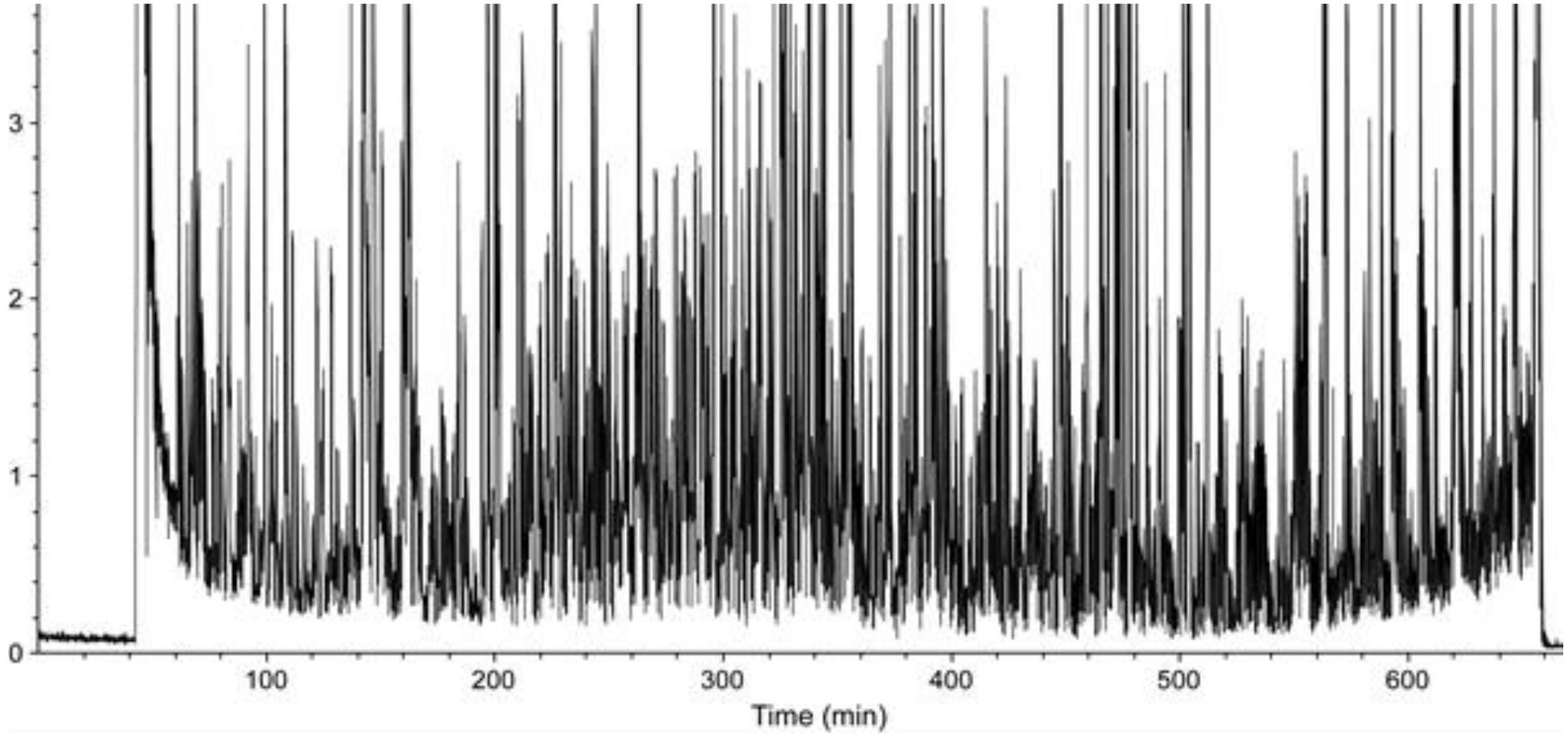

Figure 4:

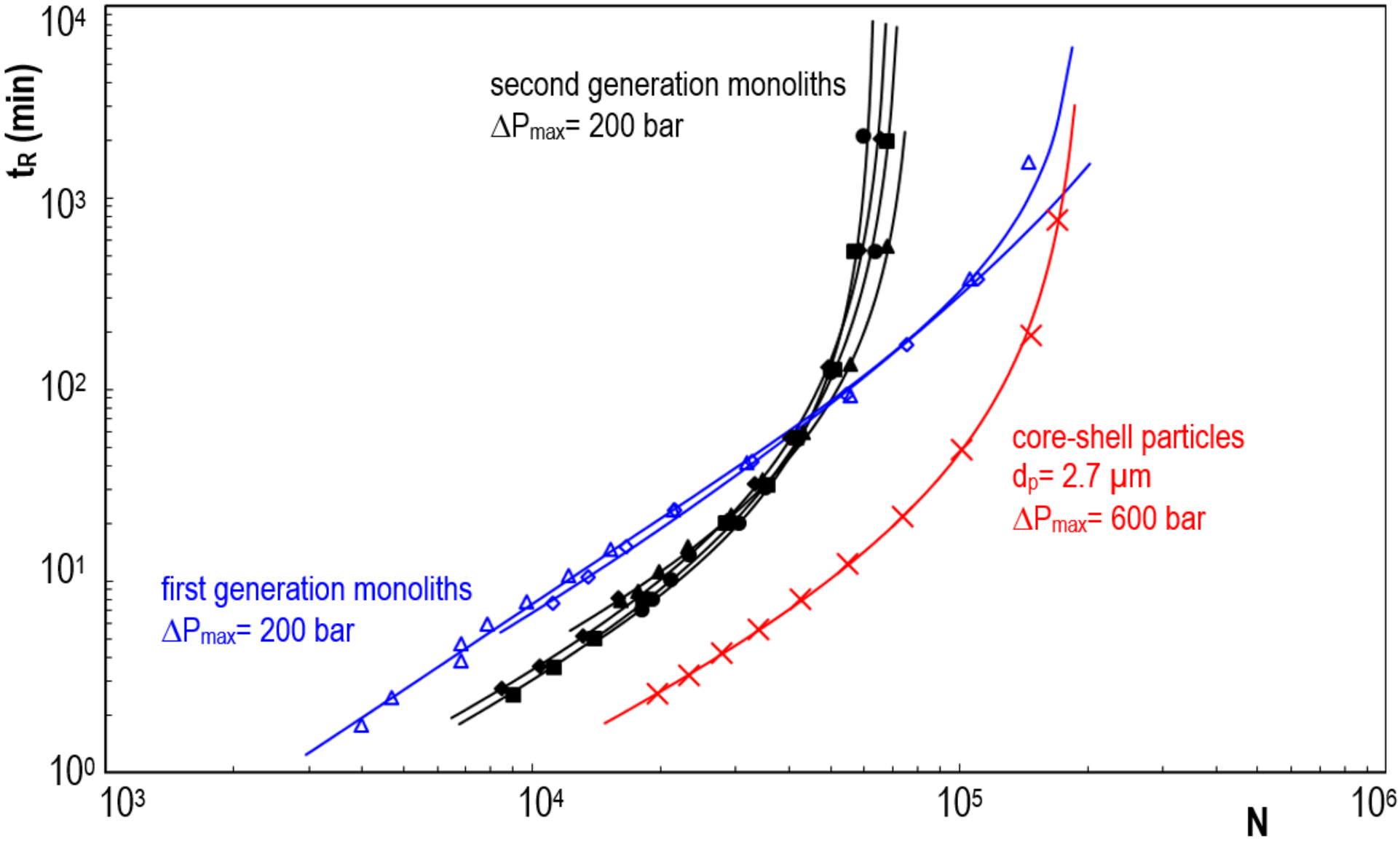
10^4
10^3
10^2
10^1
10^0
t_R (min)
second generation monoliths
ΔP_{max}= 200 bar
core-shell particles
d_p= 2.7 µm
ΔP_{max}= 600 bar
first generation monoliths
ΔP_{max}= 200 bar
10^3
10^4
10^5
10^6
N

Figure 5:

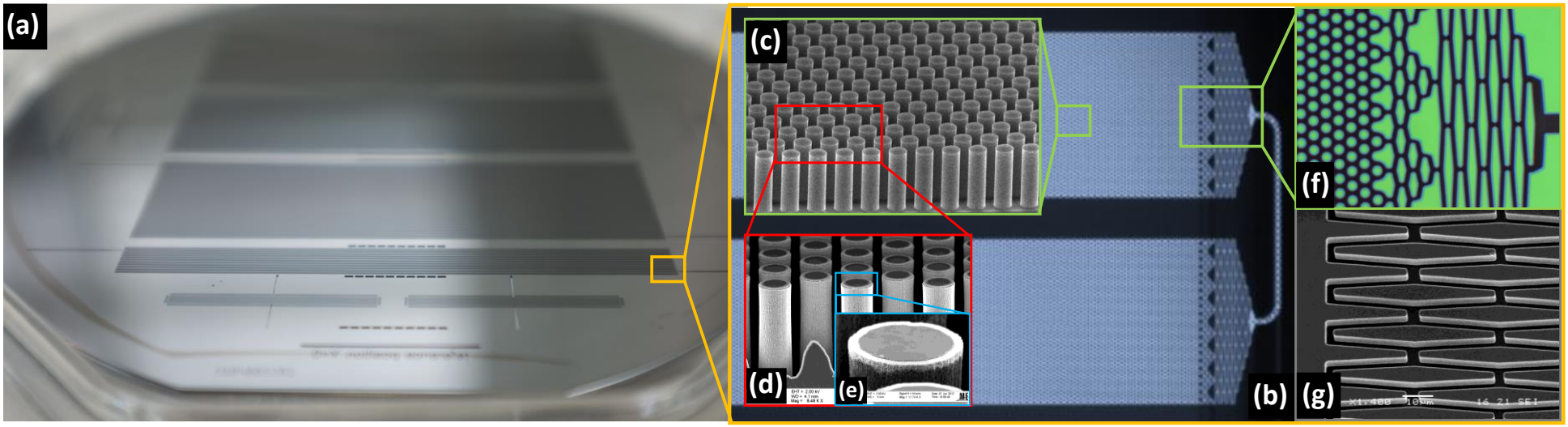

Figure 6:

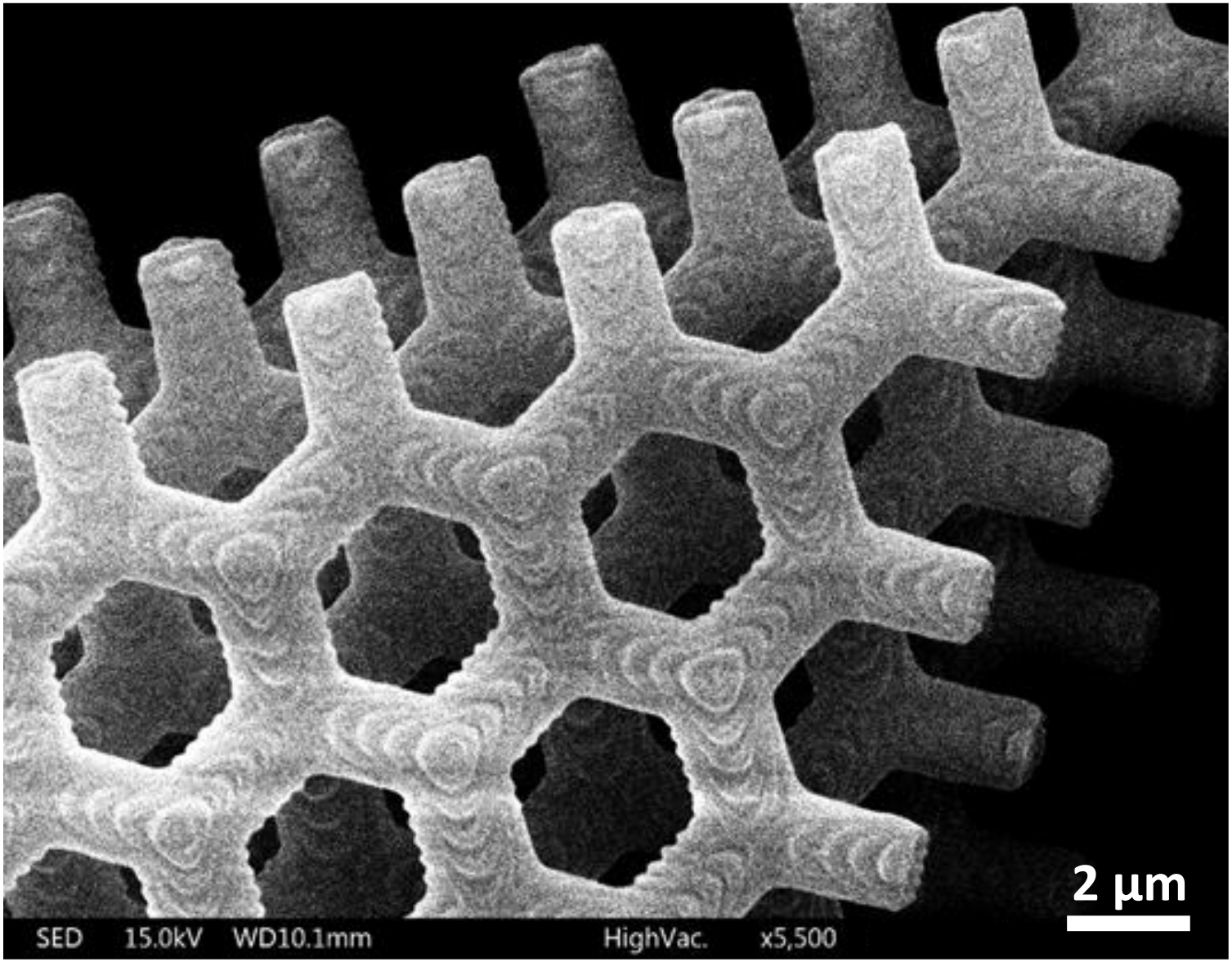

References

[1] D.R. Stoll, T.D. Maloney, Recent Advances in Two-Dimensional Liquid Chromatography for Pharmaceutical and Biopharmaceutical Analysis, LCGC North America 35 (2017) 680-687.

[2] D.R. Stoll, K. Shoykhet, P. Petersson, S. Buckenmaier, Active Solvent Modulation: A Valve-Based Approach To Improve Separation Compatibility in Two-Dimensional Liquid Chromatography, Anal. Chem. 89 (2017) 9260-9267.

[3] M. Pursch, S. Buckenmaier, Loop-Based Multiple Heart-Cutting Two-Dimensional Liquid Chromatography for Target Analysis in Complex Matrices, Anal. Chem. 87 (2015) 5310-5317.

[4] K. Sandra, M. Steenbeke, I. Vandenheede, G. Vanhoenacker, P. Sandra, The versatility of heart-cutting and comprehensive two-dimensional liquid chromatography in monoclonal antibody clone selection, J. Chromatogr. A 1523 (2017) 283-292.

[5] K. Broeckhoven, J. De Vos, G. Desmet, Particles, Pressure, and System Contribution: The Holy Trinity of Ultrahigh-Performance Liquid Chromatography, LC GC Eur. 30 (2017) 618-625.

[6] M. Golay, Theory of chromatography in open and coated tubular columns with round and rectangular cross-sections, in: D.H. Desty (Editor), Gas Chromatography 1958, Butterworths, London, 1959, p. 36.

[7] J.H. Knox, M. Saleem, J. Chromatogr. Sci. 7 (1969) 614.

[8] S. Jespers, K. Broeckhoven, G. Desmet, Comparing the Separation Speed of Contemporary LC SFC, and GC, LC GC Eur., 30 (2017) 284-291.

[9] J. Billen, G. Desmet, Understanding and design of existing and future chromatographic support formats, J. Chromatogr. A, 1168 (2007) 73–99.

[10] R.E. Majors, Current Trends in HPLC Column Usage, LCGC North America 30 (2012) 20-34.

[11] O.H. Ismail, M. Catani, L. Pasti, A. Cavazzini, A. Ciogli, C. Villani, D. Kotoni, F. Gasparrini, D.S. Bell, Experimental evidence of the kinetic performance achievable with columns packed with new 1.9 µm fully porous particles of narrow particle size distribution, J. Chromatogr. A 1454 (2016) 86-92.

[12] M. Catani, O.H. Ismail, A. Cavazzini, A. Ciogli, C. Villani, L. Pasti, C. Bergantin, D. Cabooter, G. Desmet, F. Gasparrini, D.S. Bell, Rationale behind the optimum efficiency of columns packed with new 1.9 µm fully porous particles of narrow particle size distribution, J. Chromatogr. A 1454 (2016) 78-85.

[13] Understanding the Science Behind Packing High-Efficiency Columns and Capillaries: Facts, Fundamentals, Challenges, and Future Directions, F. Gritti, M.F. Wahab, LCGC North America 36 (2018) 82-98.

[14] R. Henry, Impact of Particle Size Distribution on HPLC Column Performance, LCGC N. Am. 32 (2014) 12–19.

[15] J.M. Godinho, A.E. Reising, U. Tallarek, and J.W. Jorgenson, J. Chromatogr. A 1462 (2016) 165–169.

[16] D. Cabooter, J. Billen, H. Terryn, F. Lynen, P. Sandra, G. Desmet, Detailed characterisation of the flow resistance of commercial sub-2µm reversed-phase columns, J. Chromatogr. A, 1178 (2008) 108–117.

[17] D. Cabooter, A. Fanigliulo, G. Bellazzi, B. Allieri, A. Rottigni, G. Desmet, Relationship between the particle size distribution of commercial fully porous and superficially porous high-performance liquid chromatography column packings and their chromatographic performance, J. Chromatogr. A 1217 (2010) 7074-7081.

[18] D.V. McCalley, Some practical comparisons of the efficiency and overloading behaviour of sub-2 µm porous and sub-3 µm shell particles in reversed-phase liquid chromatography, J. Chromatogr. A 1218 (2011) 2887–2897.

[19] Y. Vanderheyden, D. Cabooter, G. Desmet, K. Broeckhoven, Isocratic and gradient impedance plot analysis and comparison of some recently introduced large size core–shell and fully porous particles, J. Chromatogr. A 1312 (2013) 80–86.

[20] T.-C. Wei, A. Mack, W. Chen, J. Liu, M. Dittmann, X. Wang, W.E. Barber, Synthesis characterization, and evaluation of a superficially porous particle with unique, elongated pore channels normal to the surface, J. Chromatogr. A 1440 (2016) 55–65.

[21] S. Deridder, M. Catani, A. Cavazzini, G. Desmet, J. Chromatogr. A, 1456 (2016) 137–144.

[22] A. Tiselius, Chromatographic analysis - General introduction, Disc. Faraday Soc. 7 (1949) 7-11.

[23] T. Hara, S. Futagami, S. Eeltink, W. De Malsche, G. V. Baron, G. Desmet, Very High Efficiency Porous Silica Layer Open-Tubular Capillary Columns Produced via in-Column Sol–Gel Processing, Anal. Chem. 88 (2016) 10158-10166.

[24] Futagami, S., Hara., T., Ottevaere, H., Baron, G.V., De Malsche, W., Preparation and evaluation of mesoporous silica layers on radially elongated pillars, Journal of Chromatography A, 1523 (2017) 234-241.

[25] F. Detobel, H. Eghbali, S. De Bruyne, Herman Terryn, H. Gardeniers, G. Desmet, Effect of the presence of an ordered micro-pillar array on the formation of silica monoliths, J. Chromatogr. A 1216 (2009) 7360-7367.

[26] N. Tanaka, H. Kobayashi, K. Nakanishi, H. Minakuchi, N. Ishizuka, A new type of chromatographic support could lead to higher separation efficiencies, Anal. Chem. 73 (2001) 420A-429A.

[27] H. Minakuchi, K. Nkanishi, N. Soga, N. Ishizuka, N. Tanaka, Effect of domain size on the performance of octadecylsilylated continuous porous silica columns in reversed-phase liquid chromatography, J. Chromatogr. A 797 (1998) 121-131.

[28] J. Billen, P. Gzil, G.V. Baron, G. Desmet, Journal of Chromatography A, 1077 (2005) 28–36.

[29] J. Billen, P. Gzil, G. Desmet, Anal. Chem., 78 (2006) 6191-6201.

[30] F. Svec, J.M.J. Fréchet, Continuous rods of macroporous polymer as high-performance liquid chromatography separation media, Anal. Chem. 64 (1992) 820-822.

[31] Q.C. Wang, F. Svec, J.M.J Fréchet, Macroporous polymeric stationary-phase rod as continuous separation medium for reversed-phase chromatography, Anal. Chem. 65 (1993) 2243-2248.

[32] S. Wouters, T. Hauffman, M.C. Mittelmeijer-Hazeleger, G. Rothenberg, G. Desmet, G.V. Baron, S. Eeltink, Comprehensive study of the macropore and mesopore size distributions in polymer monoliths using complementary physical characterization techniques and liquid chromatography, J. Sep. Sci. 39 (2016) 4492-4501.

[33] C. Viklund, F. Svec, J.M.J. Fréchet, K. Irgum, Monolithic, “Molded”, porous materials with high flow characteristics for separations, catalysis, or solid-phase chemistry: control of porous properties during polymerization, Chem. Mater. 8 (1996) 744-750.

[34] E.C. Peters, F. Svec, J.M.J. Fréchet, C. Viklund, K. Irgum, Control of porous properties and surface chemistry in “molded” porous polymer monoliths prepared by polymerization in the presence of TEMPO, Macromolecules 32 (1999) 6377-6379.

[35] A. Vaast, H. Terryn, F. Svec, S. Eeltink, Nanostructured porous polymer monolithic columns for capillary liquid chromatography of peptides, J. Chromatogr. A 1374 (2014) 171-179.

[36] S. Eeltink, S. Wouters, J.L. Dores-Sousa, F. Svec, Advances in organic polymer-based monolithic column technology for high-resolution liquid chromatography-mass spectrometry profiling of antibodies, intact proteins, oligonucleotides, and peptides, J. Chromatogr. A 1498 (2017) 8-21.

[37] A. Premstaller, H. Oberacher, C.G. Huber, High-performance liquid chromatography-electrospray ionization mass spectrometry of single- and double stranded nucleic acids using monolithic capillary columns, Anal. Chem. 72 (2000) 4386-4393.

[38] S. Eeltink, B. Wouters, G. Desmet, M. Ursem, D. Blinco, G.D. Kemp, A. Treumann, High-resolution separations of protein isoforms with liquid chromatography time-of-flight mass spectrometry using polymer monolithic capillary columns, J. Chromatogr. A 1218 (2011) 5504-5511.

[39] S. Eeltink, S. Dolman, F. Detobel, R. Swart, M. Ursem, PJ. Schoenmakers, High-efficiency liquid chromatography – mass spectrometry separations with 50 mm, 250 mm, and 1 m long polymer-based monolithic capillary columns for the characterization of complex proteolytic digests, J. Chromatogr. A 1217 (2010) 6610-6615.

[40] R.D. Arrua, E.F. Hilder, Highly ordered monolithic structures by directional freezing and UV-initiated cryopolymerization. Evaluation as stationary phases in high performance liquid chromatography, RSC Adv. 5 (2015) 71131-71138.

[41] R.D. Arrua, A. Nordborg, P.R. Haddad, E.F. Hilder, Monolithic cryopolymers with embedded nanoparticles. I. Capillary liquid chromatography of proteins using neutral embedded nanopoarticles, J. Chromatogr. A 1273 (2 013) 26-33.

[42] Nischang, I. Taedale, O. Bruggeman, J. Chromatogr. A 1217 (2010) 7514-7522.

[43] K. Nakanishi, N. Soga, Phase separation in silica sol-gel system containing polyacrylic acid. I. Gel formation behavior and effect of solvent composition, J. Non-Cryst. Sol. 139 (1992) 1-13.

[44] K. Nakanishi, N. Soga, Phase separation in silica sol-gel system containing polyacrylic acid. II. Effects of molecular weight and temperature, J. Non-Cryst. Sol. 139 (1992) 14-24.

[45] T. Hara, S. Eeltink, G. Desmet, J. Chromatogr. A 1446 (2016) 164–169.

[46] Miyamoto, K., Hara, T., Kobayashi, H., Morisaka, H., Tokuda, D., Horie, K., Koduki, K., Makino, S., Núñez, O., Yang, C., Kawabe, T., Ikegami, T., Takubo, H., Ishihama, Y., Tanaka, N., Anal. Chem. 80 (2008) 8741.

[47] D.V. McCalley, Comparison of conventional microparticulate and a monolithic reversed-phase column for high-efficiency fast liquid chromatography of basic compounds, J. Chromatogr. A 965 (2002) 51-64.

[48] F. Gritti, G. Guiochon, Measurement of the eddy diffusion term in chromatographic columns. I. Application to the first generation of 4.6 mm I.D. monolithic columns, J. Chromatogr. A 1218 (2011) 5216-5227.

[49] D.T.-T. Nguyen, D. Guillarme, S. Heinisch, M.-P. Barrioulet, J.-L. Rocca, S. Rudaz, J.-L. Veuthey, J. Chromatogr. A 1167 (2007) 76

[50] R.E. Majors, LC–GC N. Am. 23 (2005) 1248.

[51] J.E. MacNair, K.C. Lewis, J.W. Jorgenson, Anal. Chem. 69 (1997) 983.

[52] K. Morisato, S. Miyazaki, M. Ohira, M. Furuno, M. Nyudo, H. Terashima, K. Nakanishi, Semi-micro-monolithic columns using macroporous silica rods with improved performance, J. Chromatogr. A 1216 (2009) 7384-7387.

[53] S. Altmaier, K. Cabrera, Structure and performance of silica-based monolithic HPLC columns, J. Sep. Sci. 31 (2008) 2551-2559.

[54] F. Gritti, G. Guiochon, Measurement of the eddy dispersion term in chromatographic columns: III. Application to new prototypes of 4.6 mm I.D. monolithic columns, J. Chromatogr A 1225 (2012) 79-90.

[55] D. Cabooter, K. Broeckhoven, R. Sterken, A. Vanmessen, I. Vandendael, K. Nakanishi, S. Deridder, G. Desmet, Detailed characterization of the kinetic performance of first and second generation silica monolithic columns for reversed-phase chromatography separations, J. Chromatogr. A 1325 (2014) 72-82.

[56] S. Deridder, S. Eeltink, G. Desmet, Computational study of the relationship between the flow resistance and the microscopic structure of polymer monoliths, J. Sep. Sci. 34 (2011) 2038-2046.

[57] R.E. Majors, Future Needs of HPLC and UHPLC Column Technology, LCGC North America 33 (2015) 886-887.

[58] T. Hara, G. Desmet, G. V. Baron, H. Minakuchi,S. Eeltink, Effect of polyethylene glycol on pore structure and separation efficiency of silica-based monolithic capillary columns, J. Chromatogr. A 1442 (2016) 42–52.

[59] S. Fekete, D. Guillarme, Kinetic evaluation of new generation of column packed with 1.3µm core–shell particles, J. Chromatogr. A 1308 (2013) 104-113.

[60] He, B.; Tait, N.; Regnier, F. E. Anal. Chem. 70 (1998) 3790–3797.

[61] Regnier, F. E. J. High Resolut. Chromatogr. 23 (2000) 19–26.

[62] De Malsche, W., Eghbali, H., Clicq, D., Vangelooven, J., Gardeniers, H. and Desmet, G, Pressure-driven reverse-phase liquid chromatography separations in ordered nonporous pillar array columns, Anal. Chem., 79 (2007) 5915-5926.

[63] Op De Beeck, J., De Malsche, W., Tezcan, S.T., De Moor, P., Van Hoof, C., Desmet, G., Impact of the limitations of state-of-the-art microfabrication processes on the performance of pillar array columns for LC, J. Chromatogr. A, 1239 (2012) 35-48.

[64] Op De Beeck, J., Callewaert, M., Ottevaere, H., Gardeniers, H., Desmet, G., De Malsche, W., On the advantages of radially elongated structures in microchip-based liquid chromatography, Anal. Chem., 85 (2013) 5207-5212.

[65] Op De Beeck, J., Callewaert, M., Ottevaere, H., Gardeniers, H., Desmet, W., De Malsche, W., Suppression of the side-wall effect in pillar array columns with radially elongated pillars, Journal of Chromatography A, 1367 (2014) 118-122.

[66] Desmet, G. Callewaert, M., Ottevaere, H., De Malsche, W., Merging open-tubular and packed bed liquid chromatography, Analytical Chemistry, 87 (2015) 7382–7388.

[67] Callewaert, M., Op De Beeck, J., Maeno, K., Sukas, S., Thienpont, H., Ottevaere, H., Gardeniers, H., Desmet, G., De Malsche, W., Integration of uniform porous shell layers in very long pillar array columns using electrochemical anodization for liquid chromatography, Analyst, 139 (2014) 618-625.

[68] Isokawa, M., Takatsuki, K., Song, YT, Shih, K., Nakanishi, K., Xie, ZM, Yoon, DH, Sekiguchi, T, Funatsu, T, Shoji, S, Tsunoda, M., Liquid Chromatography Chip with Low-Dispersion and Low-Pressure-Drop Turn Structure Utilizing a Distribution-Controlled Pillar Array, Anal. Chem. 88 (2016) 6485-6491.

[69] De Malsche, W., Clicq, D., Verdoold, V., Gzil, P., Desmet, G. and Gardeniers, H., Integration of porous layers in ordered pillars for liquid chromatography, Lab Chip 7 (2007) 1705-1711.

[70] De Malsche, W., Zhang, L., Op De Beeck, J., Vangelooven, J., Majeed, B., Desmet, G., Micron-sized pillars for ion-pair reversed-phase DNA separations, J. Sep. Sci., 33 (2010) 3613-3618.

[71] Op De Beeck, J., De Malsche, W., De Moor, P., Desmet, G., HDC separations in micro-and nanopillar arrays produced using deep-UV lithography, J. Sep. Sci., 35 (2012) 1877-1883.

[72] De Malsche, W., De Bruyne, S., Op De Beeck, J., Sandra, P., Gardeniers, H., Desmet, G., Lynen, Capillary LC separations using non-porous pillar array columns, J. Chromatogr. A, 1230 (2012) 41-47.

[73] De Malsche, W., Op De Beeck, J., De Bruyne, S., Gardeniers, H., Desmet, G. (2012), The realization of $1 \cdot 10^6$ theoretical plates in liquid chromatography using very long pillar array columns, Anal chem., 84, 1214-1219.

[74] Waheed, S., Cabot, J.M., Macdonald, N.P., Lewis, T., Guijt, R.M., Paull, B., Breadmore, M.C., 3D printed microfluidic devices: enablers and barriers, Lab on a Chip, 16 (2016) 1993-2013.

[75] Sandron, S., Heery, B., Gupta, V., Collins, D.A., Nesterenko, E.P., Nesterenko, P.N., Talebi, M., Beirne, S., Thompson, F., Wallace, G.G., Brabazon, D., Regan, F., Paull, B., 3D Printed metal columns for capillary liquid chromatography, Analyst 139 (2014) 6343-6347.

[76] Fee, C., Nawada, S., Dimartino, S., D printed porous media columns with fine control of column packing morphology, J. Chromatogr. A., 1333 (2014) 18-24.

[77] Nawada, S., Dimartino, S., Fee, C., Dispersion behavior of 3D-printed columns with homogeneous microstructures comprising differing element shapes, Chem. Eng. Sci., 164 (2017) 90-98.

[78] Emons, M., Obata, K., Binhammer, T., Ovsianikov, A., Chichkov, B.N., Morgner, U., Two-photon polymerization technique with sub-50 nm resolution by sub-10 fs laser pulses, Optical Materials Express, 2 (2012) 942.